www.DeepakPublishing.com

Kim, S. et al. (2018): JoSS, Vol. 7, No. 1, pp. 701–717
(Peer-reviewed article available at www.jossonline.com)

www. JoSSonline.com

Design, Fabrication, and Testing of an Electrical Double-Layer Capacitor-Based 1U CubeSat Electrical Power System

Tamer Aburouk, Sangkyun Kim, Hirokazu Masui, and Mengu Cho

Kyushu Institute of Technology, Kitakyushu
Fukuoka, Japan

Abstract

At the present time, rechargeable batteries such as Li-ion or Ni-CAD are widely used in CubeSat Electrical Power Subsystems (EPS) as a power source in the absence of sunlight because of their many advantages, including their compact size and the amount of energy they can store. However, robustness, simplicity, reliability, safety, and reduction of the overall failure rate of the EPS must also be considered as requirements for CubeSat EPS in harsh space environments. These requirements can be addressed, however, by eliminating the batteries and using an Electrical Double-Layer Capacitor (EDLC)-based 1U CubeSat EPS, as described in this paper. A new EDLC-based EPS board was developed and tested in this study for its electrical performance and robustness in space environments, including launch environments and thermal environments. The total EDLC capacitance was 1600 F, the EPS occupying a volume of 90 × 87.3 × 64.6 mm. The functionality of the board was tested, assuming realistic power, voltage, and current profiles based on actual orbital periods, and assuming release of the satellite from the International Space Station (ISS). The CubeSat power consumption profile was assumed to be from 920 mW to 2.67 W, and the photovoltaic power generation output to be 2.93 W, at its peak. The board was proven to withstand space environments, and to provide the power to operate a CubeSat in orbit, with a remaining energy level of 52% at the end of eclipse.

1. Introduction

CubeSats are built for simple, basic missions to support space research and experiments, space education, and data exchange; however, the commercial sector is also increasingly interested in their use. At this time, CubeSats are mainly developed at universities and institutes and by small companies, because of their low cost, short building time, small sizes, reliability, and mass, and they are most commonly put into orbit from the International Space Station (ISS), or launched on rockets as a secondary payload (Mehrparvar, 2014). However, as technology and reliability improve, and access to the space environment increases (presenting higher orbit possibilities), the useful life of CubeSats is also enhanced, foreseeably attracting more interest in their use from larger-scale commercial businesses and emerging companies.

Such developments are in progress. New launch capabilities can accommodate larger sized satellites, including up to 1 × 6U, 2 × 3U, or even 2 × 6U. In addition, double-wide deployers are now available, as are piggy-backed opportunities for both single-wide

Corresponding Author: kim.sangkyun571@mail.kyutech.jp
Publication History: Submitted – 10/14/17; Revision Accepted – 04/30/18; Published – 06/08/18

and double-wide systems that stay with the upper stage for higher orbit deployment, rather than connecting with the International Space Station (ISS). Increasingly complex, useful design objectives are becoming more common, as users and developers are finding realistic ways to meet profitable and valuable mission goals. The design and testing of a new Electrical Double-Layer Capacitor (EDLC)-based 1U Cubesat Electrical Power Systems (EPS) described in this paper is another such development.

A CubeSat's EPS has complete power distribution elements, including power generation, voltage step-up (or -down), power storage, protection, voltage step-down (or -up), and a distribution unit. Figure 1 shows a schematic diagram of a generic EPS used in many CubeSats.

Solar arrays are the main component for power generation, connected in series and parallel to generate the required voltages and currents. The DC/DC converter is used to change the output voltage and charge the batteries. Rechargeable batteries are used for energy storage and as a secondary source of electrical power for operation during eclipse periods. The rechargeable batteries always require a protection unit to avoid overcharging, and required operating temperature must be maintained. DC/DC voltage regulators regulate and step the bus voltage down or up to 3.3 V, 5 V, or other levels for different subsystems. A pin port is used for power distribution to deliver the regulated voltages of 3.3 V and 5 V, as well as other unregulated voltages, to the different CubeSat subsystems.

Although CubeSats are usually designed for simple missions, or to run small scientific experiments under space environment conditions, they still tend to have a higher failure rate, due to components with low reliability, absence of redundancy, design complexity, unskilled workmanship, and less robust components that cannot withstand harsh space environments (i.e., radiation, wide temperature ranges, launch vibration, etc.). EPS is the major failure driver of overall CubeSat failure, contributing 28% to 44%, up to 90 days after ejection (Langer and Bouwmeester, 2016). Recognizing that rechargeable batteries are among the most fragile components in CubeSats because they have a very narrow temperature range and require considerable protection, the main purpose of this study was to design and build a robust 1U CubeSat EPS in which rechargeable batteries are replaced with EDLCs, thus providing the new EPS with the required robustness, reliability, simplicity, and safety (see Figure 2 for a block diagram). This, in turn, will increase the overall survivability rate of CubeSats, resulting in longer possible mission lifespans, higher orbital operations, and more significant mission goals. The EDLCs, also called "Ultra Capacitors" or "Super Capacitors," are electrical components capable of holding hundreds of times greater amounts of electrical charge than a standard capacitor. The cell maximum charge voltage lies between 2.5 V and 2.7 V. The EDLCs are polar components, which means they have positive and negative terminals, and are connected correctly in circuits (Capacitor Guide, 2017; A Brief History of Supercapacitors, 2007).

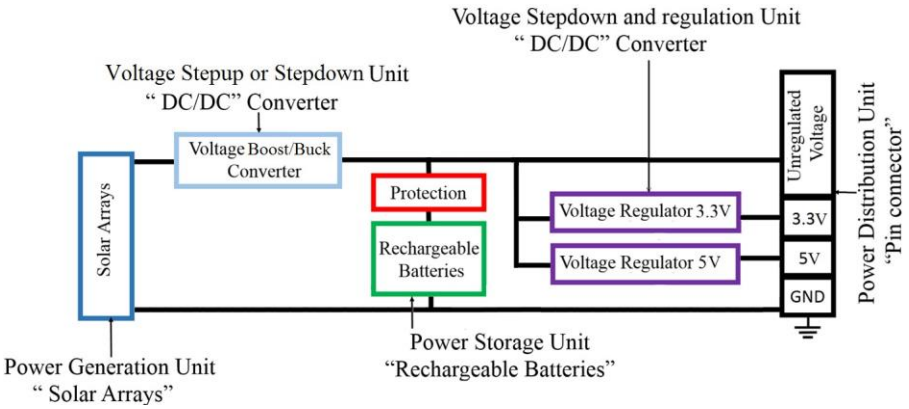

Figure 1. Typical EPS elements of a 1U CubeSat.

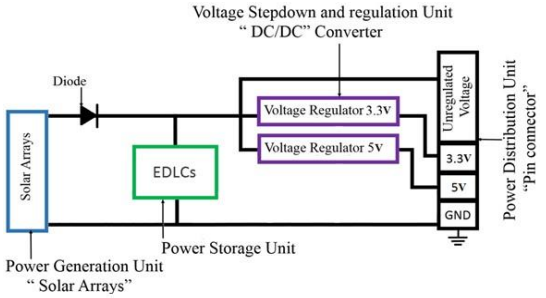

Figure 2. ELDC-based 1U CubeSat EPS block diagram.

The EDLCs provide the new EPS with the following advantages:

- *Robustness.* Long-life usage (up to 15 years); more than one million charge and discharge cycles; a wide operating temperature range (−40° C to +65° C); and strong structure.
- *Performance.* High charge and discharge rate; rapid charging; deep charge and discharge; fast transient response (~20 microseconds); high specific power; and linear discharge with constant current loads (Alkali et al., 2015).
- *Simplicity.* Simple charging method by direct energy transfer (DET); free of maintenance; easy installation; interface; fixable mounting; and a rated cell voltage of 2.7 V, which is almost equal to three-junction solar cell voltage. Comparing Figure 1 with Figure 2 shows the simplicity of the EPS after replacing the rechargeable batteries with the EDLC. However, the satellite application requirements will affect the overall design simplifications, such as the need for extra DC/DC converters, the number of EDLCs required, or the number of solar cells required.
- *Safety*. No explosive hazards, since it is free of chemical reactions; no hazard with a little overcharging or deep discharging per manufacturer recommended limits; and no protection circuits required. (Gidwani, Bhagwani, and Rohra, 2014; Faradigm, 2017). Environmentally friendly, if the capacitor is a dry type. If the capacitor contains liquid electrolyte, its toxic level must be determined, and leaking in the vacuum must be checked. Considering the fact that the capacitor can be launched in a fully discharged state, it is harmless to the launcher and other passengers, as long as no charging occurs before deployment and no leakage occurs for the case of liquid type. In the case of using liquid EDLCs, application of a Burn-in Cycling test is recommended to demonstrate the control of leakage, even for EDLCs that are launched discharged.

Table 1 shows a comparison between EDLCs and general rechargeable Li-ion batteries. Regarding the safety compliance of the EPS, an experienced integrator will be able to provide guidance early in design phase when any necessary changes can be accommodated with minimum impact.

A previous study (Alkali, Edries, and Cho, 2015) introduced the idea of implementing EDLCs in an EPS system in replacement of rechargeable batteries, laboratory testing and verifying an EDLC for space application usages. Focusing only on the EDLC itself, the study verified its functionality through charge and discharge cycles, and mechanical vibra-

Table 1. EDLC & Li-ion Battery Comparison (Gidwani, Bhagwani, and Rohra, 2014)

Function	EDLCs	Li-ion batteries (general)
Charge time	1–10 sec	10–60 min
Life cycles	1 million cycles or 30,000 hours	500 cycles and higher
Cell rated voltage	2.3 to 2.75 V	3.6 to 3.7 V
Specific energy (Wh/Kg)	5 (typical)	100 to 200
Specific power (W/Kg)	up to 10,000	1000 to 3000
Cost per Wh	20 $ (typical)	2 $ (typical)
Service life	10 to 15 years	5 to 10 years
Charge temperature	−40 to +65° C	0 to +65° C
Discharge temperature	−40 to +65° C	−20 to +60° C

tion, vacuum, thermal vacuum, and thermal cycle tests were performed. The purpose of the present paper is to report the results obtained in a more advanced stage of this research, in which an EPS circuit board was designed and fabricated to be fit into a 1U CubeSat. The circuit was tested for various environmental factors, and the EPS board was tested under a realistic load profile based on a real orbital period, using a simulated Solar Array Simulator (SAS).

This paper is composed of five parts: After the introduction (the first section), the second part will explain the design steps, the challenges, and the advanced components used to build the system. The third part recounts the calculation of the exact sunlight and eclipse periods, and derivation of estimates of the generated power of the proposed CubeSat solar cells. This section then describes the first functional test, as well as tests on mechanical vibration, vacuum, and thermal cycles. System functionality (excluding vibration) was checked after each test. In the fourth section, generated voltages, currents, and load profiles are described based on real orbital periods, and conclusions are presented in the fifth section.

2. Design

Figure 3 shows the final design in 3D. Designing and building the EDLC-based EPS involved various steps and challenges. The board dimension was chosen based on the assumption that the EDLC will be demonstrated in orbit using a 1U CubeSat based on the satellite bus developed for the BIRDS constellation (Monowar et al., 2017), which adopts a backplane approach proposed by the University of Wurzburg (UNISEC Europe, 2017).

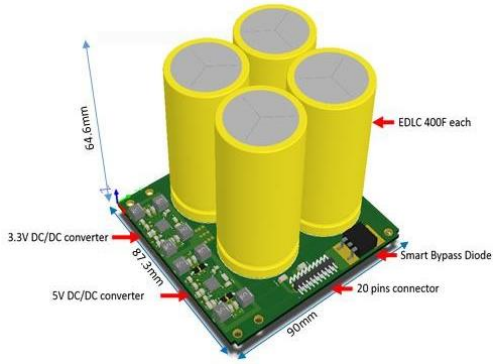

Figure 3. 3D CAD image of the whole EDLC-based EPS circuit board design.

The first challenge was selecting a proper EDLC that can fit into a small 1U CubeSat, has enough mechanical strength and rigidity to withstand the mechanical vibration during launch, and has proper mounting terminals that can be fitted easily in the printed circuit board (PCB). Thus, a dry type 400-F EDLC manufactured by Eton, shown in Figure 4, was selected for this study. The important specifications are listed in Table 2. The total size of the EDLC-based EPS circuit board is 90 × 87.3 mm, to fit into a 1U CubeSat structure. Therefore, only four of the mentioned EDLCs can be installed on it, and the new EDLC-based EPS occupies from 60% to 70% of the CubeSat's overall volume. The four EDLCs are all connected in parallel, so that they can provide the maximum possible capacitance of 1600 F, while the rated voltage is still 2.7 V.

Figure 4. Eaton 400-F EDLC, used in the study.

Table 2. Specifications of the EDLC Used in the Study

Specifications		
1	Manufacturer	Eaton
2	Capacitance	400 F
3	Working Voltage	2.7 V
4	Surge Voltage	2.85 V
5	Capacitance Tolerance	-5% to +10%
6	Operating Temperature	-40° C to +65° C
7	Equivalent Series Resistance	3.2 mΩ
8	Typical Mass	72 g
9	Dimensions	ϕ = 35 mm, L = 60 mm

The second challenge was regulating the low voltages of the EDLC (2.7 V and below) to 3.3 V and 5 V, with high-output continuous current. Different DC/DC boost converters have been used, but all of them failed to provide sufficient output current for

high-load power requirements such as data transmission or mission operation. Finally, a DC/DC boost controller (LTC3425) from Linear Technology was selected. It has a greater than 95% converting efficiency, up to 3 A continuous output current, and an input voltage up to 0.5 V. We chose a DC/DC converter capable of working up to the very low voltage, because we may need to exploit any power remaining at EDLC, even if the photovoltaic power generation is not enough to sustain the satellite operation and charging.

The third challenge was reducing the voltage drop of the solar cell output voltage as much as possible, to have sufficient voltage to charge the EDLCs up to their nominal voltage of 2.7 V without using a DC/DC converter. Usually, in EPS systems, a Schottky diode is used between solar cells and the downstream part of the EPS, to prevent any back current from the downstream to the solar cells. However, Schottky diodes are not suitable for this novel EDLC-based EPS system, due to a voltage drop as high as 450 mV, while the maximum generated voltage by solar cells is only 2.7 V, since all the solar cells are connected in parallel. If a Schottky diode were used, the voltage after the diode would not be sufficient to charge EDLCs up to their rated voltage. Thus, the "Smart Bypass Diode SM74611," developed by Texas Instruments, was selected. This diode is characterized by its extremely low voltage drop of just 26 mV at 8 A. For the new EDLC-based EPS, a voltage drop of just 7.35 mV at maximum generated a current of 2.26 A. Figure 5 shows the voltage drop curves against current and at different temperatures.

A 20-pin connector LPC-20m2LG, developed by HTK, was used to distribute the power to different

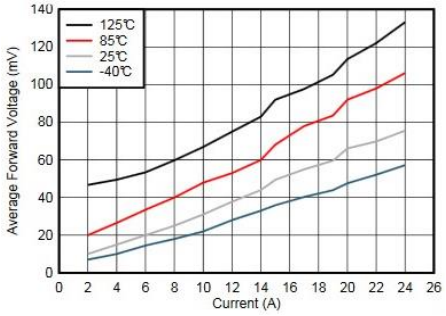

Figure 5. Voltage drop against current and in different temperatures (Texas Instruments SM74611, 2016).

subsystems, and combine the solar cell output power to charge the EDLCs. Figure 6 shows the connector pin assignment.

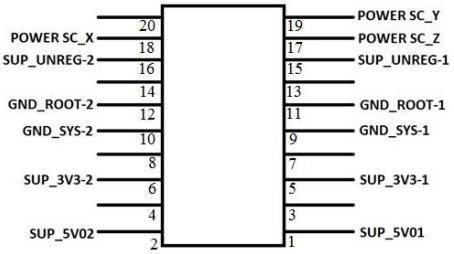

Figure 6. LPC-20m2LG 20-pin assignment.

Pin 1 and Pin 2 deliver a 5-V regulated voltage in parallel. In the present paper, the two outputs are connected together. Pins 3 and 4 are free pins. Pin 5 and Pin 6 deliver a 3.3-V regulated voltage in parallel, and are also connected together. Pins 7 and 8 are free pins. Pin 9 and Pin 10 are connected to the system ground. Pins 11 and 12 are connected to the root ground. The root ground is the ground of the solar cells, and the system ground is the ground of the load side. Pins 9, 10, 11, and 12 are all connected, and Pins 13 and 14 are free pins. Pin 15 and Pin 16 deliver EDLC unregulated voltage. Pins 17, 18, and 19 receive power from the solar cells. They are connected to the EDLCs and the voltage input of the LTC3425. In the present paper, the output of the external power supply was connected to each of Pins 17, 18, and 19. Finally, Pin 20 is a free pin. By selecting the proper EDLCs, DC/DC converters, and diodes, we were able to complete the design and fabricate the final circuit board for testing. Figure 3 shows the final circuit in 3D before fabrication. Table 3 summarizes the total configurations of the EDLC-based EPS.

3. Environment Testing

To achieve the aim of this study and verify that the new system is suitable for space applications, various environmental tests were performed, namely, a mechanical vibration test, a vacuum test, and a thermal cycle test. Before and after each test, a functional test was repeated to ensure that no problems occurred during the test. For a specific hardware to be selected

Table 3. General Configurations of EDLC-based EPS

	Description	*Value*
1	Dimensions	X87.3 mm × Y90 mm × Z64.6 mm
2	Total Mass	Approx. 300 g
3	Total Capacitance	1600 F
4	No. of EDLCs	4
5	PCB no. of layers	2
6	PCB type	FR-4
7	Maximum input voltage	2.7 V
8	Regulated Voltages	5 V, 3.3 V
9	Unregulated voltage	2.7 V and less
10	Maximum Output Current at regulated voltage 3.3 V	2.8 A at EDLC 2.7 V
11	Maximum Output Current at regulated voltage 5 V	2.5 A at EDLC 2.7 V
12	Maximum voltage drop	Approx. 7.35 mV at smart bypass diode
13	Number of components	54 elements
14	Total Cost	Approx. $230, including final board fabrication

by a satellite system integrator for flight, it is expected that the hardware passes the tests mentioned here and the test reports will be provided.

3.1. Functional Tests

Functional testing of the system consisted of an EDLC charging test, an EDLC discharging test, and DC/DC boost converter output voltage testing. This study also calculated the total capacitance and deviation from the rated value.

3.1.1. Solar Array Simulator

We developed a simulated triple-junction solar cell using the LabVIEW® program, and implemented it in various tests, replacing expensive commercial Solar Array Simulator (SAS) devices, and without the use of real three-junction solar cells. With this simulated solar cell, we were able to control a normal DC power supply through DAQ connection to behave as a solar array, with the same environmental conditions of LabVIEW® (Jaleel, Nazar, and Omega, 2012; Rezka and Hasaneen, 2015).

The simulated solar cell has a generic specification of triple-junction solar cells often used in CubeSat projects. Its specifications are: Isc = 0.6 A, Voc = 2.7 V, Pm = 1.25 W at Imp = 0.5 A and Vmp = 2.5 V, Temp = 25° C, and Area = 0.0032 m^2 (Gonzalez-Llorente et al., 2015). Figure 7 shows the simulated

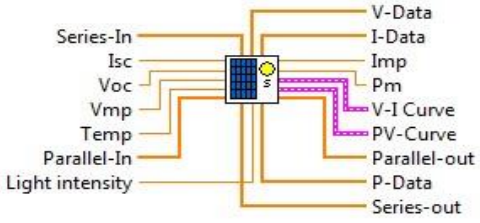

Figure 7. Simulated LabVIEW-based SAS.

LabVIEW-based SAS with all input and output parameters.

The power generated by solar cells can be calculated with Equation (1), as follows:

$$P = A \times S \times \eta \times cos\theta\ . \qquad (1)$$

A: Solar cell area, equaling 0.0032 m^2
S: Light intensity, equaling 1400 W/m^2
η: Solar cell efficiency, equaling 28%
θ: Angle between a sunlight beam and the solar cell surface.

θ can be calculated by Equation (2):

$$\theta(top) = 90 - \big(\beta + (90 - i)\big). \qquad (2)$$

i: inclination angle of the CubeSat
β: Beta angle

The present study assumes for simplicity that two faces of a CubeSat, each having two solar cells, are constantly illuminated by sunlight at a 45° incident

angle. Then, the generated power is 2.93 W, if cells are operated at the maximum power point of I-V curve. It further assumes that all the cells are connected in parallel. Then we obtain the I-V curve shown in Figure 8. The output of the SAS follows the I-V curve defined by the maximum power, Pm. An example is shown in Figure 9, which gives the I-V

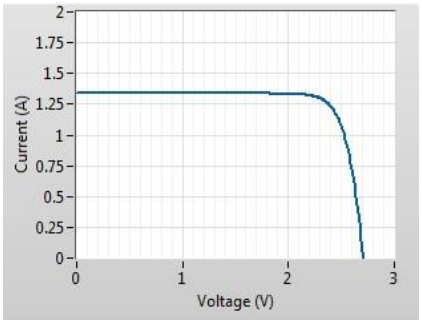

Figure 8. V-I curve assuming 2.93 W peak power.

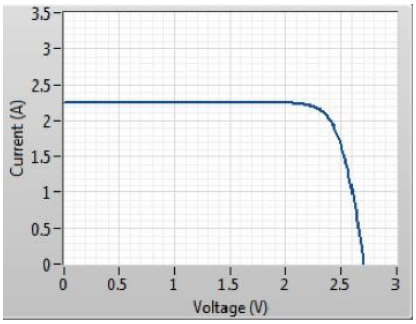

Figure 9. V-I curve assuming 4.98 W peak power.

curve of Pm=2.93 W. In this case, the specification of I-V curve is as follows: Isc = 1.34 A, Voc = 2.7 V, Pm = 2.93 W at Vmp = 2.34 V, and Imp = 1.28 A. The solar simulator provides the voltage and the current according to the IV curve, depending on the power demand from EDLC and the satellite load. Therefore, the power is not fixed at the peak power point. During the functional test, assuming a realistic operation profile of a CubeSat described in Section 4, we used the I-V curve shown in Figure 8. The assumption of 2.93 W may be a little high for a typical CubeSat, but the result shown in Section 4 indicates that there is still a margin in the solar cell generated power to support the simple CubeSat mission described there.

During the EDLC charging testing described below, we assume an I-V curve defined by 4.98 W peak power, shown in Figure 9. The power of 4.98 W is chosen from the maximum power obtained by a CubeSat when its three surfaces are illuminated by the sunlight.

3.1.2. EDLC Charging Test

The purpose of the EDLC charging test was to check the maximum rated voltage and total charging time, and observe any distortions in the voltage charging curve to insure the quality of these commercial types of EDLCs. The circuit was connected as shown in Figure 10. A PC with LabVIEW simulated SAS was connected with a power supply device through DAQ (A), to control it to behave as an SAS.

Results:

Figure 11 shows the EDLC charging voltage and curve with the simulated SAS. The voltage increased from 0.29 V to 2.66 V, while the charging current started at 2.26 A and ended with 0.25 A. The total charging time was 36.56 minutes. From the results, it was observed that the EDLCs were charged successfully by LabVIEW-based SAS. Also, from the graph, it can be noted that there are no distortions in the curves, which proves that the EDLCs are of good quality and free of manufacturing defects.

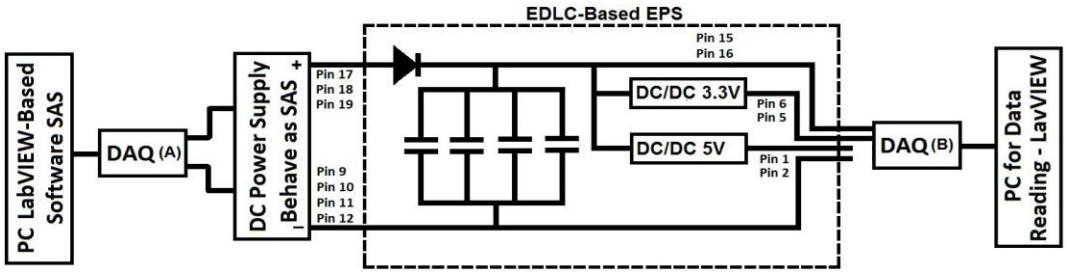

Figure 10. Typical circuit for EDLC charging test.

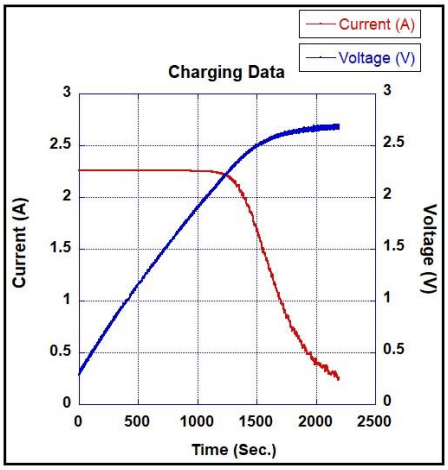

Figure 11. EDLC charging voltage and current curves, using simulated LabVIEW-based SAS.

3.1.3. EDLC Discharging Test

The purposes of the EDLC discharging test were to measure the capacitance, the deviation from the rated value, and the total discharging time, and to observe unforeseen odd distortions in discharging curves to check the EDLC quality and manufacturing defects. The circuit was connected as shown in Figure 12. First, EDLCs were charged up to their rated voltage. Then, the electronic load device was connected with the PC through DAQ to monitor and record EDLC discharge data with LabVIEW software.

Results:

Figure 13 shows the discharge curves of the EDLC voltage and current, using an electronic load device with a 1A constant current (CC) configuration. The voltage changed from 2.49 V at the start to 0 V at the end. The discharge current was 1A constant, and the total discharge time was 64.42 minutes.

Equation (3) is used to calculate the EDLC capacitance by discharge curve (ELNA, 2011):

$$C = \frac{I \times T}{(V_0 - V_1)} \quad (3)$$

I: Discharge constant current value = 1 A
V_0: First voltage reading = 2 V
V_1: Second voltage reading = 1 V
T: Discharge time between V_0 and V_1 = 1612 s

By substituting the upper values in equation (3), the capacitance C = 1612 F. The deviation can be calculated by Equation (4), as follows:

$$Deviation = \frac{Tested\ Capacitance - Rated\ Capacitance}{Rated\ Capacitance} \times 100\% \quad (4)$$

From the results, it can be noted that the total discharge time is 64.42 minutes, which is longer than a typical eclipse time in LEO. This means that the EDLCs will be able to provide power with 1 A during an eclipse period without running out of charge. The EDLC capacitance is 1612 F, which is very close to the rated capacitance of 1600 F. Deviation from the rated value is 0.75%, which is in the range of −5% to +10% suggested by the manufacturer (PowerStore XV series, 2014). From the discharge curve, no odd distortions can be seen, indicating that the EDLCs are of good quality and free of manufacturing defects.

3.1.4. EDLCs Discharging with 3.3-V or 5-V DC/DC

The purposes of the EDLC discharging test with each of the DC/DC converters was to check the functionality of the converter chips, the total regulation time, and the minimum input voltages provided by the EDLCs to keep the DC/DC converters functioning. The circuit was connected as shown in Figure 14,

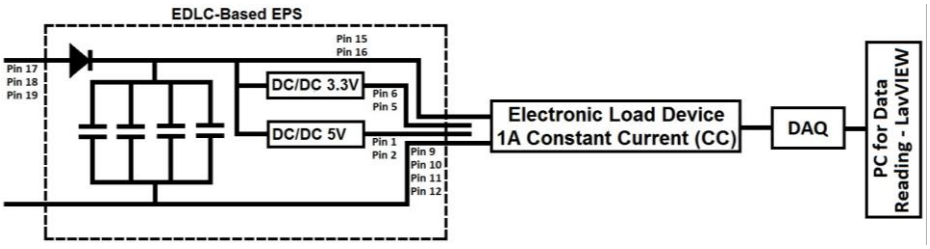

Figure 12. Typical circuit for EDLC discharging test.

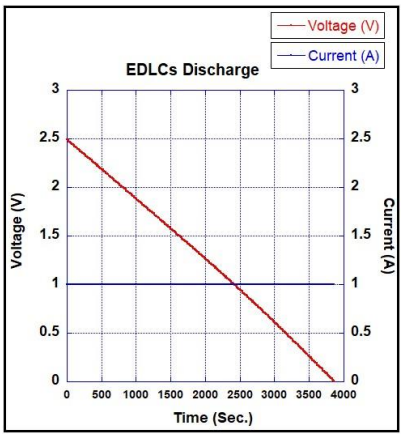

Figure 13. EDLCs, discharging voltage and current curves.

which shows the case of testing 3.3-V. After the EDLCs were charged up to their rated voltage, the electronic load device was connected with the PC through DAQ to monitor and record EDLC discharge data with LabVIEW software. Then same test was repeated, connecting the load with 5-V DC/DC.

Results:

The results of the DC/DC converters tests are summarized in Table 4.

Figure 15 shows the regulated output voltage and current of a 3.3-V DC/DC converter. A continuous current of 0.33 A was required to run a 1-W load power consumption. Figure 16 shows the regulated output voltage and current of a 5-V DC/DC converter. The continuous current was 0.22 A. From the results, it can be seen that the 3.3-V DC/DC converter keeps regulating the voltage and current and delivers a 1 W constant power to the load for 60.15 mins, which is far longer than an eclipse period. When the EDLC voltage reached 0.64 V, the discharge stopped. For the case of the 5-V DC/DC converter, the EDLCs supplied 1 W of power to the load for 53.35 minutes, which is also far longer than an eclipse period. When the EDLC voltage reached 0.81 aV, the discharge stopped.

3.2. Mechanical Vibration Test

The purpose of this test was to evaluate the impact of the vibration induced by a launch vehicle on the EDLC-based EPS circuit board and its electronics. In this test, the standards of ISO-19683, "Space Systems - Design Qualification and Acceptance Tests of Small Spacecraft and Units," were followed. As shown in Figure 17, the EDLC-based EPS was installed on the shaker of the vibration machine, and on all axes (X, Y, Z), we applied a signature check (identification of resonant frequencies), random vibration, sinusoidal, and then a signature check again. After completing all of the vibration tests on all axes, a functional test was repeated to verify the functionality of the system, and these steps are listed in Figure 18. The vibration machine input parameters for the signature check is listed in Table 5. For the random vibration and the sinusoidal vibration, see Table 5 of ISO-19683, which gives the minimum test level and duration for unit qualification test that guarantee that a given unit has a certain level of tolerance against the space environment. For a specific launcher condition, an experienced integrator is required to provide guidance in required levels of vibration spectra for the EDLCs, which may be different or more severe than the structural requirements of the satellite.

The vibration test, which used Eaton EDLCs, was satisfactory, and no anomalies were observed. No cracks or damage on the PCB were found, no loose or broken parts, no shift in toque mark, no cracks in the soldered parts, no disconnection of the lead wire to the EDLCs, and no peeling of the bonded part. No significant shift in natural frequency through any axis was observed. The functional test results showed no signs of anomalies. Figure 19 shows the EDLCs discharge curves.

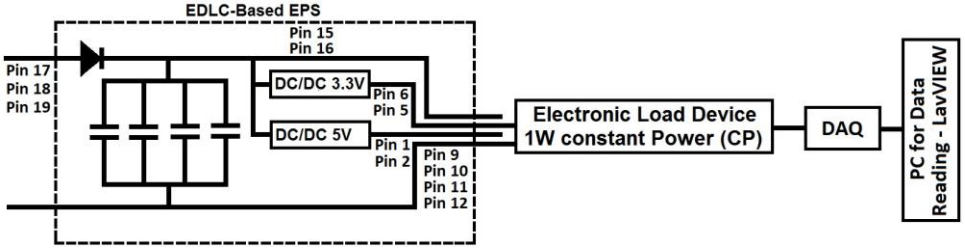

Figure 14. Typical circuit for EDLC discharging test with 3.3-V DC/DC converter.

Table 4. DC/DC Converter Functional Test Results

S/N	*Description*	*3.3-V DC/DC Test*	*5-V DC/DC Test*
1	EDLC Starting Discharge Voltage	2.51 V	2.51 V
2	EDLC Final Voltage	0.64 V	0.81 V
3	DC/DC Regulated Voltage	3.3 V	4.99 V
4	DC/DC Continuous Current	0.33 A	0.22 A
5	Total Regulated Time	60.15 mins	53.35 mins

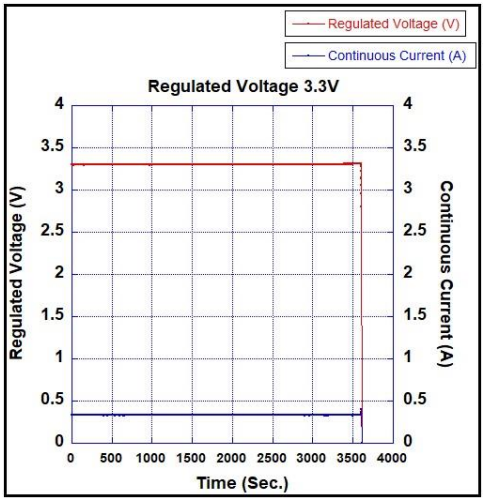

Figure 15. Regulated voltage and current curves with 3.3-V DC/DC boost converter.

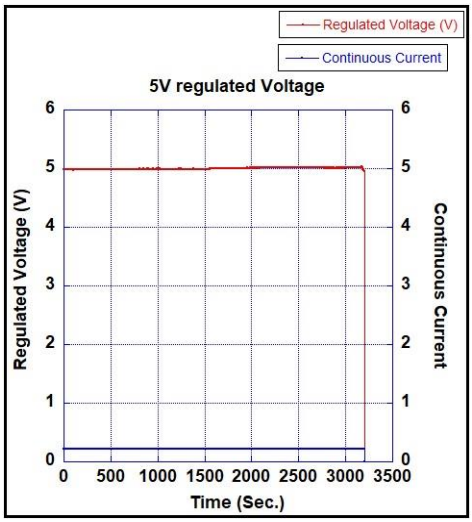

Figure 16. Regulated voltage and current curves with 5-V DC/DC boost converter.

Before it was decided to use Eaton EDLCs, other EDLCs had been selected for this study. These, manufactured by AEROGEL, failed in the mechanical vibration test. They showed significant changes in

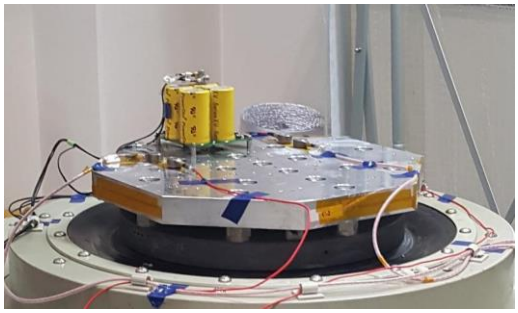

Figure 17. EDLC-Based EPS on vibration machine Z-axis.

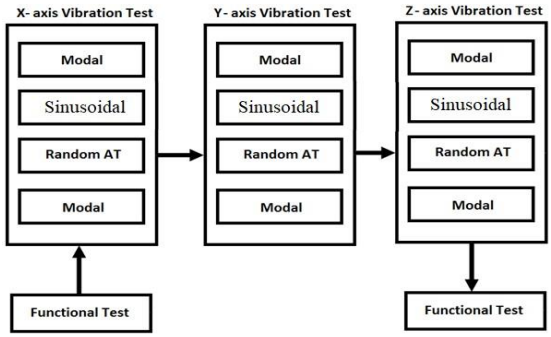

Figure 18. Mechanical vibration test flow chart.

Table 5. Signature Check Test Input Parameters

Signature Check			
Direction	Frequency [Hz]	Acceleration [Grms]	Time [min]
X,Y,Z	5~2000	0.5	1

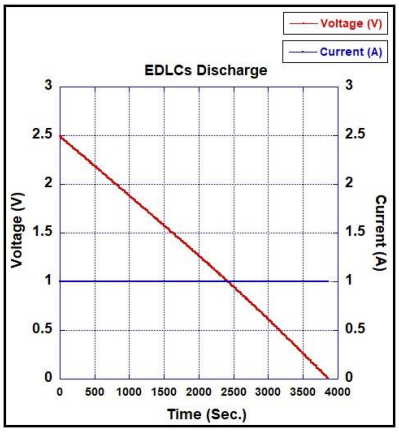

Figure 19. Successful Eaton EDLC's discharge curves.

natural frequency, and a sound indicating internal damage in the EDLCs was heard. The functional tests failed to provide values within the range. Figure 20 shows the EDLC discharge curves with odd distortion on the voltage curve, and Table 6 lists the results of the failed functional tests.

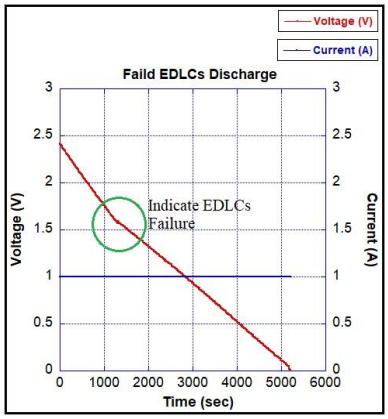

Figure 20. Failed AEROGEL EDLCs discharge curves.

The external appearance of Eaton EDLCs and those made by AEROGEL was very similar. Both of the same shape, color, and size, they were manufactured under the PowerStore brand name, with the early models manufactured by AEROGEL, and the recent models, by Eaton. Eaton EDLCs have more mechanical strength in the casing, with surrounding stripes in the middle of the case that can be seen under the external yellow sheet.

3.3. Vacuum Test

The purpose of this test was to check the functionality of the EDLC-based EPS in a vacuum environment, but at room temperature. The EPS was exposed to vacuum with a pressure of 4×10^{-4}Pa for 24 hours. Figure 21 shows the vacuum chamber used for this experiment. The EDLC-based EPS circuit board was installed inside the aluminum box. No anomalies were observed, and the functional test results showed no signs of anomalies.

3.4. Thermal Cycle Test

The purpose of this test was to check the EDLC-based EPS performance at the high and low temperature limits, to check its susceptibility to the temperature cycle, and to detect latent defects of workmanship and circuit board design. Table 7 summarizes the test parameters, and Figure 22 shows the number of cycles, soaking periods, and maximum and minimum temperature. The test parameters were chosen from ISO-19683. Figure 23 shows the thermal cycle chamber used for this experiment. The results of the functional tests conducted during the thermal cycle are shown in Table 8. No anomaly was found.

3.5. Functional Tests Before, During and After the Environmental Tests

Table 8 lists the results of all functional tests, total capacitance, deviation, and outputs of DC/DC regulators before and after each environmental test. The deviation of the capacitance is from −2.5% to +0.81% of the rated value, which is within the range for acceptable variation. The regulated voltages by DC/DC converters do not deviate much. For the 3.3-V DC/DC converter, they are from 3.26 V to 3.31 V, and for the 5-V DC/DC converter, from 4.98 V to 5.02 V, also within the range for acceptable variation.

4. Functional Test with a Realistic Operation Profile at a Minimum Generated Power

4.1. Sunlight Periods and Load Consumption

Because the new EDLC-based 1U CubeSat EPS will be used in future 1U CubeSat missions, this study investigated whether it can supply enough power under realistic conditions in orbit. A CubeSat in ISS orbit was assumed, with the same orbital parameters as the ISS, a height of 415.8 km, an inclination angle of 51.64°, a right ascension angle of 177.3° at the epoch of January 1, 2016 at 12:00:00 AM UTC (Wolframalpha, 2016). A simulation was run to cal-

Table 6. Functional Test Results of Eaton's EDLCs and the Failed AEROGEL EDLCs

	Description	Value (Eaton)	Value (AEROGEL)	Range
1	Capacitance	1580 F	2214 F	1520 F ~ 1920 F
2	Deviation	-1.25%	38.37%	-5% ~ +10%
3	3.3 DC/DC regulated voltage	3.28 V	3.32 V	around 3.3 V
4	5 DC/DC regulated voltage	5.00 V	5.01 V	around 5 V

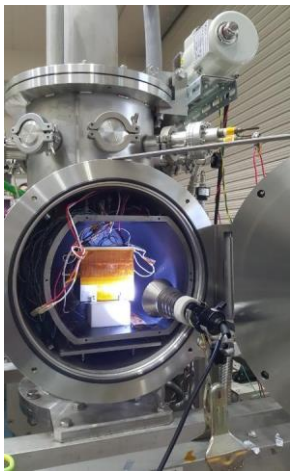

Figure 21. Vacuum chamber used for the study.

Table 7. Thermal Cycle Test Parameters

	Description	Value
1	Maximum temperature	+60° C
2	Minimum temperature	−35° C
3	No. of cycles	2 hot, 2 cold
4	Soaking period	2 h
5	Temperature ramp rate	2° C/min

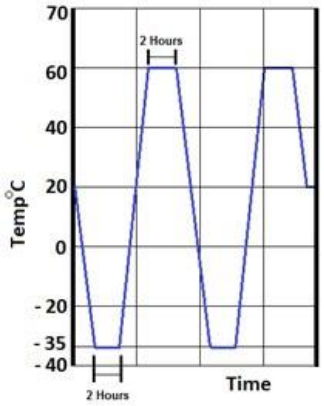

Figure 22. Chamber temperature curve.

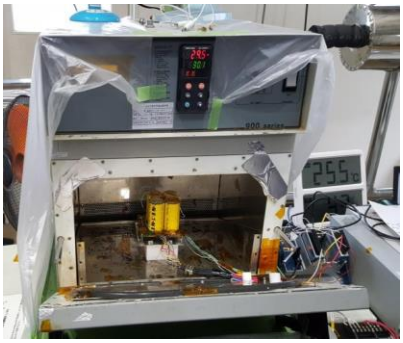

Figure 23. EDLC-based EPS inside the thermal cycle chamber.

culate the sunlight and eclipse periods. During the year, the shortest sunlight period is 57 minutes. These durations were selected for this study to check the capability of EDLCs for providing the required power during the worst case of power generation. The power generation profile was assumed to follow the I-V curve shown in Figure 8 for the sunlit time of 57 minutes.

To build a realistic power profile, it is important to calculate the power consumed by each subsystem in the proposed CubeSat, and for both sunlight and eclipse periods. Table 9 summarizes the load consumption and the working scenario for each subsystem. The assumed CubeSat mission is to take a picture and send the image via a transmitter. From Table 4, the proposed CubeSat load consumption during eclipse is 0.92 W, and the load consumption with sunlight is 0.97 W. The load consumption during mission operation (camera shot) is 1.33 W. The load consumption during data transmission is 2.67 W. Table 10 summarizes the complete configuration of the proposed CubeSat.

4.2. Functional Test

One of the study objectives was to generate realistic voltage, current, and load profiles for the EDLC-based EPS based on actual orbital periods and conditions. The profiles were generated with simulation software developed by LabVIEW®. The circuit is connected as shown in Figure 24. All the tests were performed using the I-V curve shown in Figure 8 with the peak power output of 2.93 W. The SAS output voltage, current, and power change according to the power demand from the load, as shown in Figures 25 and 26. If the generated power goes below that, there is no sufficient current to charge EDLCs and run other subsystems, at least for the first sunlight periods, as shown in Figures 27 and 28.

Figure 25 shows the temporal profiles of SAS generated current and voltage, which is also equal to the voltage of the EDLCs. The circled numbers have the following meanings:

Table 8. Results of Functional Tests

S/N	Description	Before All	After Mechanical Vibration	During Vacuum	After Vacuum	Thermal Cycle				After Thermal Cycle	Range
						1st Cold Cycle	1st Hot Cycle	2nd Cold Cycle	2nd Hot Cycle		
1	Capacitance (F)	1612	1612.9	1580	1603	1598	1583	1560	1576	1587	1520 ~ 1760
2	Deviation from 1600 F (%)	0.75	0.81	-1.25	0.19	-0.13	-1.10	-2.50	-1.50	-0.81	−5 ~ +10
4	Regulated 3.3 V output (V)	3.33	3.31	3.28	3.3	3.26	3.26	3.27	3.26	3.29	3.1 ~ 3.4
5	Regulated 5 V output (V)	4.99	5.02	5.00	5.02	5.00	4.98	5.00	4.98	4.98	4.8 ~ 5.1

Table 9. Subsystems, Functions, Usage Period, Load Consumption and Working Periods for Each Subsystem

	Subsystem	Function	Usage Period	Eclipse Load (W)	Sunlight Load (W)	Working Period (min)
1	Communication	Beacon	Full Period	0.25	0.25	Full Time
		Receiver	Full Period	0.2	0.2	Full Time
		Transmitter	Sunlight		1.7	10
2	Mission	Camera	Sunlight		0.36	5
3	Onboard Computer	Com	Full Period	0.22	0.22	Full Time
4	Power System	EPS	Full Period	0.25	0.3	Full Time

Table 10. Summary of Proposed CubeSat Configuration

	Description	Value
1	Size	1U = 10×10×10cm
2	Mission	Camera
3	Orbit	ISS Orbit (415.8km)
4	Inclination	ISS inclination (51.64°)
5	Sunlight period	57 min
6	Eclipse period	36 min
7	Solar cell quantity	10 (2×5 faces)
8	Solar cell connection	All in parallel
11	Peak power output generated by solar cells	2.93 W
10	Vmp at maximum generated power	2.3 V
11	Imp at maximum generated power	2.16 A
12	Isc at maximum generated power	2.26 A
13	Voc at maximum generated power	2.7 V
14	Load consumption during eclipse	920 mW
15	Load consumption with sunlight	970 mW
16	Load consumption during mission operation	1.33 W
17	Load consumption during transmission	2.67 W

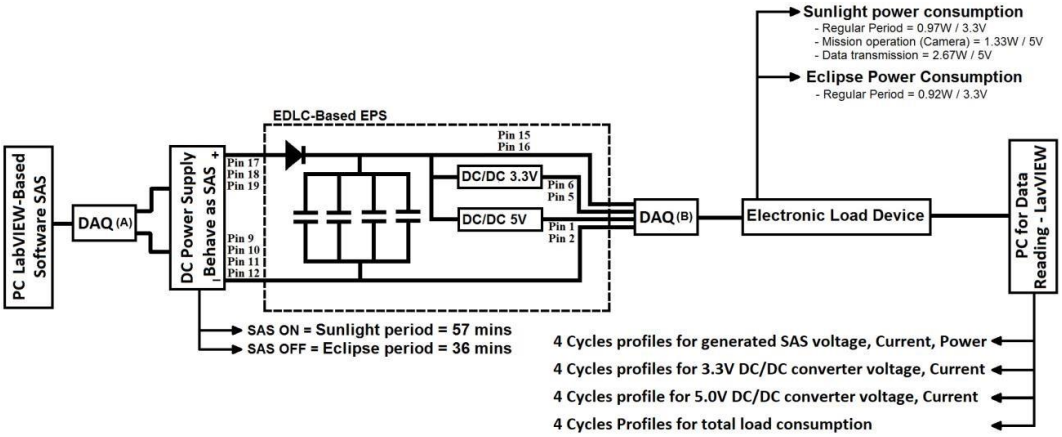

Figure 24. Complete circuit connections for profile generation at minimum generated power of 2.93 W.

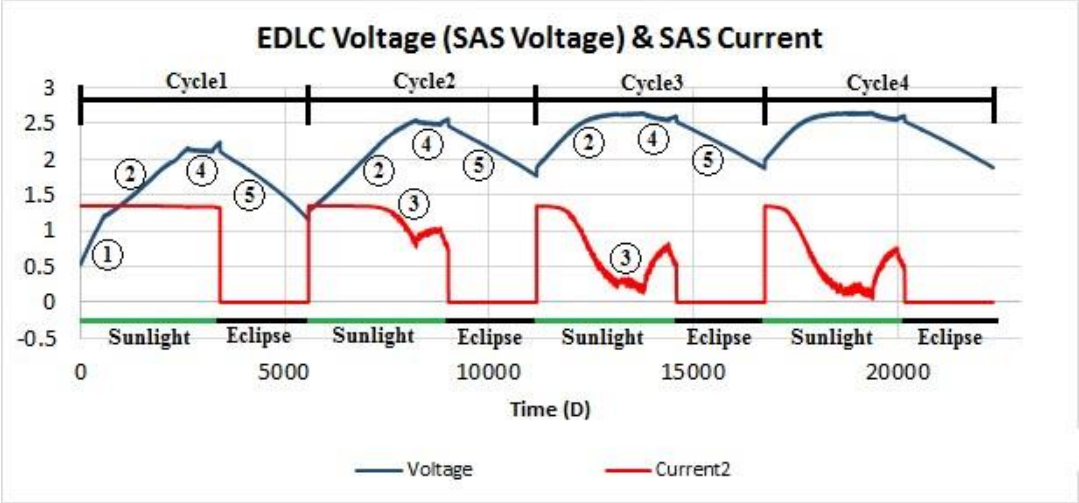

Figure 25. Four cycles of the EDLC voltage and the SAS current profile. Note that the SAS voltage is equal to the EDLC voltage.

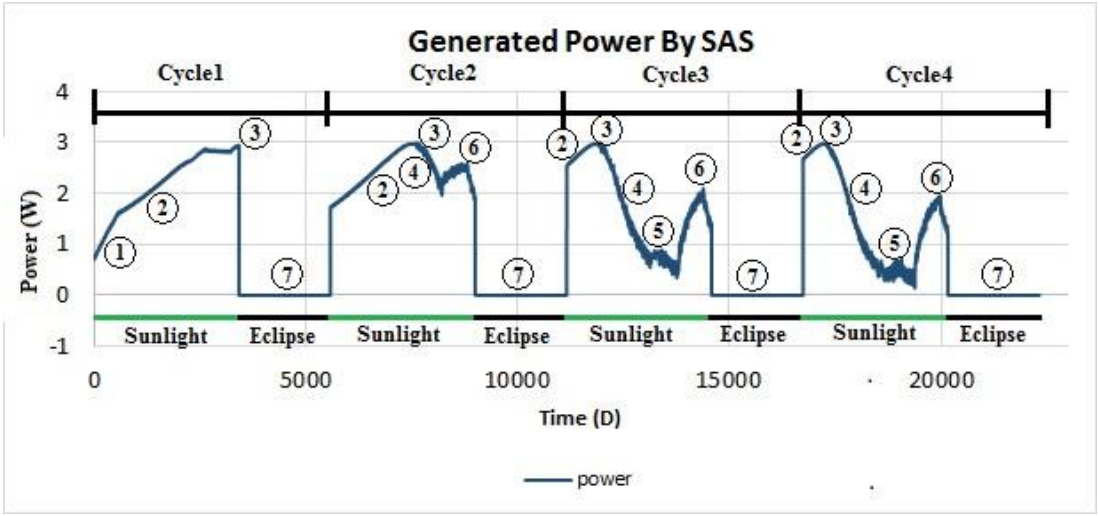

Figure 26. Four cycles of power generated by LabVIEW-based SAS.

1. EDLCs are rapidly charging. In the first cycle, and at the moment of entering a sunlight period, EDLCs have no charge, so the generated voltage is not sufficient to run the DC/DC converters to pass power to the load.
2. EDLCs keep charging up to 2.67 V. When the EDLC voltage reaches 1.1 V, the EDLCs start to feed the 3.3-V DC/DC converter and shows 0.97 W power consumption. In the second cycle, the EDLCs are fully recharged within 11.5 minutes.
3. The mission operation period for 5 minutes.
4. Data transmission period for 10 minutes.
5. EDLCs discharge during eclipse for 36 minutes, consuming the regular eclipse period load of 0.92 W, while the EDLC voltage drops to 1.95 V. The remaining energy in EDLC is 52% of the rated full energy to be stored in EDLC. This means even the solar cell output lower than 2.93 W maximum or the lower capacity of EDLC can support the CubeSat mission.

Figure 26 shows the temporal profiles of the power generated by SAS, The circled numbers have the following meanings:

1. The generated power increases rapidly while the EDLC voltage increases, and all of the generated power goes to charge the EDLCs, since the DC/DC converters are in shutdown mode because of insufficient input voltage.
2. The generated power charges the EDLCs and consumes the load of 0.97 W.
3. The generated voltage reaches the maximum and EDLCs are fully charged.
4. The generated power is reduced while the EDLC rated voltage approaches the SAS Voc. of 2.7 V.
5. The voltage generated by SAS to operate camera session for 5 minutes.
6. The power generated by SAS and EDLCs to operate the transmitter for 10 minutes.
7. No power is generated, since the CubeSat has entered the eclipse period.

Figure 27 shows the temporal profile of the 3.3-V regulated voltage and current for three cycles, starting with a sunlight period, and the EDLCs have no charge. The circled numbers have the following meanings:

1. The 3.3 V DC/DC converter is in shutdown mode. In the first cycle, the EDLCs have no charge, thus the EDLC voltage is not sufficient to run the 3.3-V DC/DC converter.
2. After 7.7 minutes, the 3.3-V DC/DC converter starts working and the regulated voltage always stays at 3.3 V.
3. The required current by regular sunlight load.
4. The required current by regular eclipse load.

Figure 28 shows the temporal profile of the 5-V regulated voltage and current for three cycles, starting with a sunlight period, and the EDLCs have no charge. The circled numbers have the following meanings:

1. The 5-V DC/DC converter is in shutdown mode. In the first cycle, the EDLCs have no charge, thus the EDLC voltage is not sufficient to run the 5-V DC/DC converter.
2. After 7.7 minutes, the 5-V DC/DC converter starts working and the regulated voltage always stays at 5 V.
3. No load, thus no current required.
4. The current required for camera mission.
5. The current required for data transmission.

Figure 29 shows the temporal profile of the total load power consumption, starting with a sunlight period, and no EDLCs have a charge. The circled numbers have the following meanings:

1. For 7.7 minutes, the EDLC-based EPS does not consume any power, because all DC/DC converters are in shutdown mode due to insufficient EDLC voltage. All power generated by SAS goes to charge the EDLCs.

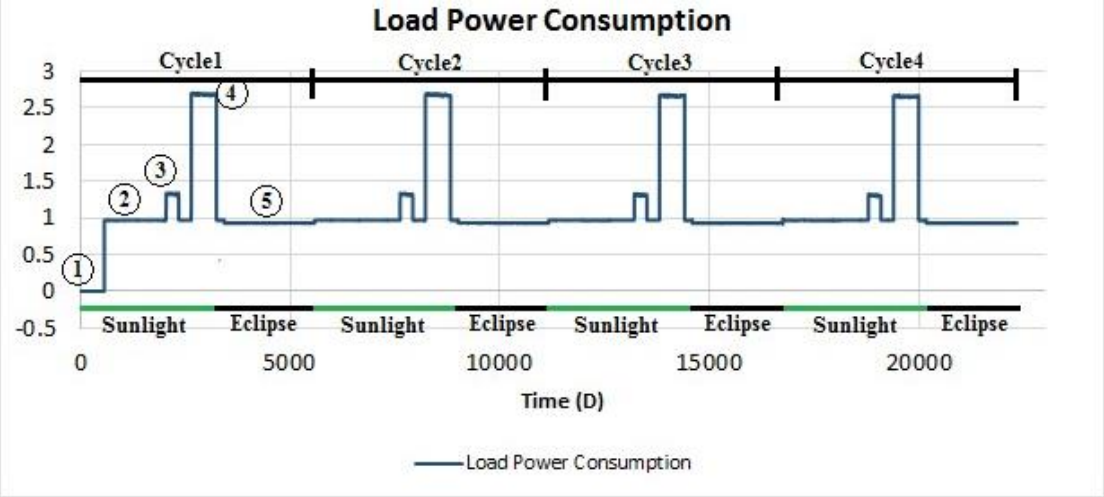

Figure 29. Three cycles of total load power consumption profiles.

2. For 57 minutes, the total power consumed during the sunlight regular period is 0.97 W.
3. For 5 minutes, the total power consumed during the mission operation is 1.33 W.
4. For 10 minutes, the total power consumed during data transmission is 2.67 W.
5. For 36 minutes, the total power consumed during the eclipse regular period is 0.92 W.

5. Conclusion

The results of the tests and profiles show that a capacitor bank of four EDLCs, each 400 F, connected in parallel, with a total capacitance of 1600 F, is suitable to build an EDLC-based EPS for a 1U CubeSat with simple missions, such as Earth imaging. The capacitor used was a dry type, posing no serious safety threat. The EPS system has a simple architecture where the output of solar array, where all the individual cells are connected in parallel providing the input voltage of 2.7 V at maximum matching, with the rated voltage of EDLC, is directly fed into the EDLC through one diode, without any regulator. The total envelope size is X87.3 mm × Y90 mm × Z64.6 mm. The functional test with a realistic operation profile of the Earth image capturing mission and the data downlink with an average power consumption of approximately 1 W showed that the EDLCs could provide the required power to all the subsystems during sunlight and eclipse periods, with the remaining energy level of 52% at the end of eclipse. The EDLC-based EPS passed the mechanical vibration, thermal cycle, and vacuum tests. During the vibration test using an early version of the EDLC, however, it was found that not all commercial EDLCs are suitable for space applications. Therefore, caution must be exercised when choosing EDLCs, considering their mechanical strength, rigidity, and size. EDLC defects manifest in the voltage curve during discharge.

Based on successful design and results, EDLCs could be accommodated individually, or in hybrid systems with batteries, to provide power for larger satellites requirements. For such a case, early interface with the launcher through the launch coordinator should reveal any design changes necessary to meet the launcher requirements. This study used the same PCB dimensions as found in the BIRDS-1 project, which employed a standard interface design for a 1U CubeSat, to increase the chance of flight opportunity. A future task is to find the soonest possible flight opportunity to carry out an on-orbit demonstration.

References

A Brief History of Supercapacitors, Batteries & Energy Storage Technology (2007): Available at: http://www.tuks.nl/pdf/Reference_Material/Electrolytic_Caps_and_Super_Caps/brief-history-of-supercapacitors.pdf (accessed July 4, 2017).

Abdul Jaleel, J., Nazar, A., and Omega, A. R. (2012): Simulation on Maximum Power Point Tracking of the Photovoltaic Module Using LabVIEW®. *Int. J. of Adv. Res. in Electrical, Electronics and Instrumentation Engineering*, Vol. 1, Issue 3 (Sept.), p. 193.

Alkali, M., Edries, M. Y., and Cho, M. (September 2015): Laboratory Verification of Electric Double Layer Capacitor Based Power System for a Simple CubeSat Mission. *Int. J. of Electrical Energy*, Vol. 3, No. 3, p. 122.

Capacitor Guide, Super Capacitors. Available at: http://www.capacitorguide.com/supercapacitor (accessed July 4, 2017).

ELNA Co. Ltd. (2011): Double Layer Capacitor Calculations. Available at: http://www.elna.co.jp/en/capacitor/double_layer/pdf/calculation.pdf (accessed July 4, 2017).

FaraDigm: Advantages of Ultra Capacitors. Available at: http://www.faradigm.com/faqs/ultracapacitors (accessed July 4, 2017).

Gidwani, M., Bhagwani, A., and Rohra, N. (2014): Supercapacitors the near Future of Batteries. *Int. J. of Engineering Inventions*, Vol. 4, Issue 5 (Oct.), pp. 22–27.

Gonzalez-Llorente, J. et al. (2015): Improving the Efficiency of 3U CubeSat EPS by Selecting Operating Conditions for Power Converters, in 2015 IEEE Aerospace Conf., Big Sky, MT US (Mar. 7-14), p. 3. Available at: https://ieeexplore.ieee.org/document/7119122/ (accessed May 16, 2018).

Honsberg, C. and Bowden, S.: Measurement of Solar Cell Efficiency (PV Education.org). Available at: http://www.pveducation.org/pvcdrom/characterisation/measurement-of-solar-cell-efficiency (accessed July 4, 2017).

ISO 19683:2017 (2017): Space Systems—Design Qualification and Acceptance Tests of Small Spacecraft and Units. Available at: https://www.iso.org/standard/66008.html (accessed September, 16, 2018).

Langer, M. and Bouwmeester, J. (2016): Reliability of CubeSats – Statistical Data, Developers' Beliefs and the Way Forward, in *Proc. 30th Ann. AIAA/USU Conf. on Small Satellites*, Logan, UT US (Aug.16, 2018). Paper No. SSC16-X-2.

Linear Technology (2003): LTC3425 Technical Datasheet 4424 (Sept, 2003). Available at: http://cds.linear.com/docs/en/datasheet/3425f.pdf (accessed July 4, 2017).

Mehrparvar, A. (2014): CubeSat Design Specifications. The CubeSat Program, CalPoly SLO.

Monowar, M. et al. (2017): BIRDS Project: Development and Operation Summary of a CubeSat Constellation Project. Presented at the 68th Int. Astronautical Cong., Adelaide, Australia, Sept. 25–29.

PowerStore XV Series (2014): Snap-in Cylindrical Supercapacitor Technical Datasheet 4424. Available at: http://www.cooperindustries.com/content/dam/public/bussmann/Electronics/Resources/product-datasheets/bus-elxds-4424-xv-series.pdf (accessed July 4, 2017).

Rezk, H. and Hasaneen, E-S. (2015): A New MATLAB/Simulink Model of Triple-Junction Solar Cell and MPPT Based on Artificial Neural Networks for Photovoltaic Energy Systems. *Ain Shams Eng. J.*, Vol. 6, Issue 3 (Sept.), pp. 873–881.

Texas Instruments (2016): SM74611 Smart Bypass Diode Technical Datasheet 4424. Available at: http://www.ti.com/lit/ds/symlink/sm74611.pdf (accessed July 4, 2017).

UNISEC Europe (2017): CubeSat Subsystem Interface Definition, version 1.0. Available at: http://unisec-europe.eu/wordpress/wp-content/uploads/CubeSat-Subsystem-Interface-Standard-V2.0.pdf (accessed March 29, 2018).

WolframAlpha Computational Knowledge Engine (2016): International Space Station Position. Available at: http://www.wolframalpha.com/input/?i=ISS+position+30+sep+2016+at+00:00 (accessed July 4, 2017).